ORIGINAL ARTICLE

FHIT, a Novel Modifier Gene in Pulmonary Arterial Hypertension

Svenja Dannewitz Prosseda[1,2], Xuefei Tian[1,2], Kazuya Kuramoto[1,2], Mario Boehm[1,2], Deepti Sudheendra[1], Kazuya Miyagawa[2,3,4], Fan Zhang[2], David Solow-Cordero[5], Joshua C. Saldivar[6], Eric D. Austin[7], James E. Loyd[7], Lisa Wheeler[7], Adam Andruska[1], Michele Donato[8], Lingli Wang[1,2], Kay Huebner[9], Ross J. Metzger[2], Purvesh Khatri[8], and Edda Spiekerkoetter[1,2,3]

[1]Division of Pulmonary and Critical Care, Department of Medicine, [2]Wall Center for Pulmonary Vascular Disease, [3]Cardiovascular Institute, [4]Department of Pediatrics, [5]High-Throughput Bioscience Center, and [6]Chemical and Systems Biology, Stanford University, Stanford, California; [7]Vanderbilt University Medical Center, Nashville, Tennessee; and [8]Biomedical Informatics Research–Institute for Immunity, Transplantation, and Infection, Stanford University, Stanford, California; [9]Molecular Genetics and Cancer Biology Program, Ohio State University, Columbus, Ohio

ORCID ID: 0000-0001-6297-4378 (S.D.P.).

Abstract

Rationale: Pulmonary arterial hypertension (PAH) is characterized by progressive narrowing of pulmonary arteries, resulting in right heart failure and death. *BMPR2* (bone morphogenetic protein receptor type 2) mutations account for most familial PAH forms whereas reduced BMPR2 is present in many idiopathic PAH forms, suggesting dysfunctional BMPR2 signaling to be a key feature of PAH. Modulating BMPR2 signaling is therapeutically promising, yet how BMPR2 is downregulated in PAH is unclear.

Objectives: We intended to identify and pharmaceutically target BMPR2 modifier genes to improve PAH.

Methods: We combined siRNA high-throughput screening of >20,000 genes with a multicohort analysis of publicly available PAH RNA expression data to identify clinically relevant BMPR2 modifiers. After confirming gene dysregulation in tissue from patients with PAH, we determined the functional roles of BMPR2 modifiers *in vitro* and tested the repurposed drug enzastaurin for its propensity to improve experimental pulmonary hypertension (PH).

Measurements and Main Results: We discovered *FHIT* (fragile histidine triad) as a novel BMPR2 modifier. BMPR2 and FHIT expression were reduced in patients with PAH. FHIT reductions were associated with endothelial and smooth muscle cell dysfunction, rescued by enzastaurin through a dual mechanism: upregulation of FHIT as well as miR17-5 repression. *Fhit*$^{-/-}$ mice had exaggerated hypoxic PH and failed to recover in normoxia. Enzastaurin reversed PH in the Sugen5416/hypoxia/normoxia rat model, by improving right ventricular systolic pressure, right ventricular hypertrophy, cardiac fibrosis, and vascular remodeling.

Conclusions: This study highlights the importance of the novel BMPR2 modifier FHIT in PH and the clinical value of the repurposed drug enzastaurin as a potential novel therapeutic strategy to improve PAH.

Keywords: pulmonary hypertension; cardiovascular diseases; enzastaurin; BMPR2; repurposed drugs

(Received in original form December 19, 2017; accepted in final form August 14, 2018)

Supported by grants from the NHLBI (K08HL107450-01 and R01 HL128734-01A1) and Pulmonary Hypertension Association/American Heart Association supplemental K08 award 2011. P.K. is funded by the Bill and Melinda Gates Foundation and by National Institute of Allergy and Infectious Diseases grants 1U19AI109662, U19AI057229, and U54I117925.

Author Contributions: S.D.P., M.B., X.T., R.J.M., K.K., K.M., and F.Z.: animal experiments. S.D.P., D.S., J.C.S., A.A., and L. Wang: functional assays. S.D.P., X.T., and D.S.-C.: high-throughout screen. M.D. and P.K.: computational analysis. E.D.A., J.E.L., and L. Wheeler: experiments with *BMPR2* mutation carriers. S.D.P. and E.S.: preparation of manuscript. E.S., S.D.P., R.J.M., K.H., E.D.A., and J.E.L.: manuscript discussion.

Correspondence and requests for reprints should be addressed to Edda Spiekerkoetter, M.D., Division Pulmonary and Critical Care, Department of Medicine, Stanford University, 300 Pasteur Drive, Stanford, CA 94305. E-mail: eddas@stanford.edu.

This article has an online supplement, which is accessible from this issue's table of contents at www.atsjournals.org.

Am J Respir Crit Care Med Vol 199, Iss 1, pp 83–98, Jan 1, 2019

Originally Published in Press as DOI: 10.1164/rccm.201712-2553OC on August 14, 2018
Internet address: www.atsjournals.org

At a Glance Commentary

Scientific Knowledge on the Subject: Familial pulmonary arterial hypertension (PAH) is most commonly caused by an underlying mutation in the *BMPR2* (bone morphogenetic protein receptor type 2) gene (~75% of cases). Reduced expression of BMPR2 occurs in both familial and idiopathic PAH, highlighting the central role of aberrant BMPR2 signaling in PAH. Modulating BMPR2 signaling can halt disease progression and presents a valuable therapeutic strategy. The objective of this study was to identify and target BMPR2 modifiers for the prevention and reversal of PAH pathogenesis.

What This Study Adds to the Field: This study presents the previously undescribed BMPR2 modifier gene *FHIT* (fragile histidine triad). The expression of FHIT is decreased in patients with PAH, and its loss *in vitro* and *in vivo* leads to the development of cellular hallmarks of PAH and experimental pulmonary hypertension (PH) in response to hypoxia. Pharmaceutical elevation of FHIT levels with enzastaurin prevents and reverses experimental PH caused by Sugen5416/hypoxia/normoxia exposure, representing a potential novel treatment strategy for PAH therapy and prevention.

Pulmonary arterial hypertension (PAH) is a devastating disease, characterized by progressive, occlusive pulmonary vasculopathy ultimately leading to right heart failure and a considerably shortened life-span. Mutations in the *BMPR2* (bone morphogenetic protein receptor type 2) gene are present in ~75% of patients with familial PAH (FPAH) (1), clearly linking *BMPR2* to the pathogenesis of the disease. Although *BMPR2* mutations and reduced BMPR2 expression were reported in many patients with idiopathic PAH (IPAH) and FPAH (2–4), surprisingly only a relatively small proportion (~20%) of *BMPR2* mutation carriers develop a clinical PAH phenotype, suggesting additional environmental or genetic factors or "second hits" involved in disease development, by either reducing BMPR2 signaling below a critical threshold or targeting BMPR2-independent pathways relevant for PAH pathogenesis.

Current PAH treatments are insufficient, as most approved PAH drugs primarily function as vasodilators or potential right ventricular (RV) stabilizers (5), leaving the pulmonary vasculopathy to progress unchecked. Therapeutic targeting of BMPR2 signaling is considered an attractive strategy to improve PAH (6–9), independent of the *BMPR2* mutational status, as our group showed with the repurposed drug FK506 that increases BMPR2 signaling (10–12). Our goal was therefore to identify and pharmaceutically target BMPR2 modifier genes to increase BMPR2 signaling or expression in patients with FPAH and IPAH.

In this study, we combined a systematic siRNA high-throughput screen (HTS) of genes that regulate BMPR2 signaling with a novel multicohort and multitissue analysis approach of publicly available PAH RNA expression. The siRNA screen identified BMPR2 activating genes that when knocked down reduced BMPR2 signaling as assessed by ID1 expression. Cross-validating these genes with genes consistently downregulated in the publicly available PAH gene expression data set allowed us to identify BMPR2 modifier genes of potential clinical relevance in PAH. We hypothesized that approaches that upregulate these genes would improve pulmonary hypertension. We identified *FHIT* (fragile histidine triad) as a potential modifier gene in PAH, showing that reduced FHIT expression was associated with reduced BMPR2 signaling and endothelial cell (EC) dysfunction *in vitro* and *in vivo*. *FHIT* is a member of the histidine triad family, located on chromosome 3, overlapping the *FRA3B* locus (13), the human common fragile site most susceptible to replication stress and associated deletions. The tumor suppressor gene *FHIT* is readily lost after exposure to carcinogens or stressors, such as cigarette smoke and ultraviolet irradiation (14, 15). FHIT is highly expressed in the lung (16) but is commonly lost in lung cancer and other malignancies (17, 18). Moreover, FHIT is implicated in apoptosis and proliferation in various cell types (19, 20), potentially linking it to the abnormal proliferative phenotype observed in PAH endothelial and smooth muscle cells (PASMCs). We show that FHIT and BMPR2 expression can be upregulated by enzastaurin, a cancer drug that appeared to be well tolerated in the context of a phase 2 clinical trial when administered for two cycles of chemotherapy for a total of ⩾56 days to prevent lymphoma relapse (21). Enzastaurin prevented and reversed experimental pulmonary hypertension (PH) progression by increasing FHIT yet also by FHIT-independent effects involving miR17-5. We propose that FHIT levels are mechanistically important in PH pathogenesis and that enzastaurin would present an ideal candidate for clinical translation. Some of the results of these studies have been previously reported in the form of an abstract (22).

Methods

A siRNA HTS of >22,000 genes using a mouse myoblastoma Id1-BRE luciferase reporter assay was used as previously described (12).

Meta-analysis of Publicly Available PAH Gene Expression Data

A novel integrated meta-analysis algorithm and a validation cohort was used to cross-validate the BMPR2 modifier genes from the mouse HTS in seven publicly available human PAH transcriptomic data sets from the National Center for Biotechnology Information Gene Expression Omnibus.

Animal Models

Adult wild-type C57BL/6, *Bmpr2*$^{+/-}$, or *Fhit*$^{-/-}$ mice at 8–10 weeks of age were housed in chronic hypoxia (10% O_2) for 3 weeks, followed by a recovery period of 4 weeks in normoxia (21% O_2). *Bmpr2*$^{+/-}$ and *Fhit*$^{-/-}$ mice and littermates were treated with a daily dose of enzastaurin (15 and 5 mg/kg/d) or vehicle for the duration of the study, administered with a mini-osmotic pump. Development of experimental PH was induced in adult Sprague-Dawley rats (8 wk old, 180–220 g) through a subcutaneous dose of the VEGFR-2 inhibitor Sugen5416 (20 mg/kg body weight), followed by exposure to chronic hypoxia (10% O_2) for 3 weeks and normoxia for 5 weeks (21% O_2), as previously described (12). SuHx rats and littermates were treated with a daily dose of enzastaurin (5 mg/kg body weight) or vehicle for 3 weeks, administered through oral gavage.

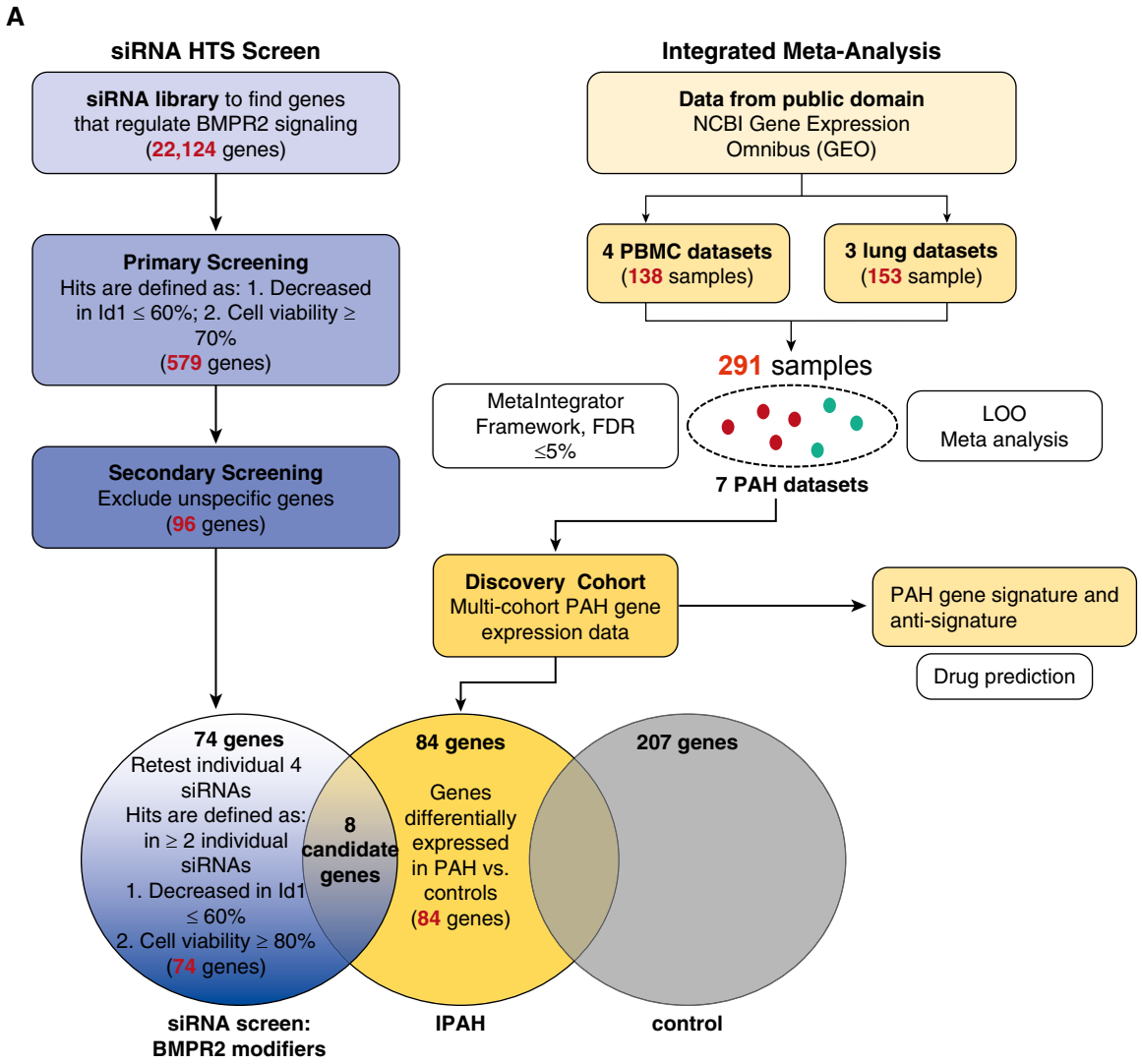

Figure 1. Identification of BMPR2 regulatory genes by a siRNA high-throughput screen (HTS) and pulmonary arterial hypertension (PAH) meta-analysis. A mouse high-throughput siRNA screen of >22,000 genes was conducted, using an Id1-BRE luciferase reporter assay in a C2C12 mouse myoblastoma cell line treated with or without 250 pM BMP4, as previously described (12). BMP4 was conducted, as previously described (12). (*A*) Targets were identified by a decrease in Id1 expression ⩽60% and viability ⩾80% in response to stimulation, yielding 74 meaningful HTS candidates. To identify a PAH signature, the candidates were validated with gene expression data from an integrated meta-analysis algorithm of PAH lung and immune cell (peripheral blood mononuclear cell) datasets and a further validation cohort. (*B*) Of eight genes that were altered in patients with idiopathic PAH, fragile histidine triad expression was most consistently downregulated throughout all data sets. (*C*) PAH gene expression profile and antisignature compared with the gene signature of enzastaurin and dasatinib. BMPR2 = bone morphogenetic protein receptor type 2; FDR = false discovery rate; FHIT = fragile histidine triad; IPAH = idiopathic PAH; LOO = leave-one-out; NCBI = National Center for Biotechnology Information; PBMC = peripheral blood mononuclear cells.

All animal experiments were approved by the Stanford University Institutional Animal Care and Use Committee.

Isolation of Cells from Human PAH Patients

Pulmonary artery ECs (PAECs) of patients with IPAH and FPAH at the time of lung transplant were obtained from digested whole-lung tissue, using CD31-AB pulldown beads as previously described (12). Peripheral blood mononuclear cells (PBMCs) were isolated from patients with PAH with negative *BMPR2* mutation status or healthy volunteers through Ficoll-Paque density gradient centrifugation (10). Lymphocytes from $BMPR2^{mut+}$ patients with PAH and their unaffected relatives were isolated from the whole blood using gradient centrifugation and subsequently virally transformed, as previously described (23).

For a detailed description of the methods, please *see* online supplement.

Results

HTS of BMPR2 Modulators and Multicohort PAH Gene Expression Assay

To find "BMPR2 modifier genes" we conducted an HTS with a murine genome-wide siRNA library (Qiagen) that included 22,124 murine genes (open reading frames), with four pooled siRNAs for each gene using the BRE-Id1-Luc reporter cell line as previously described (12) as a readout for

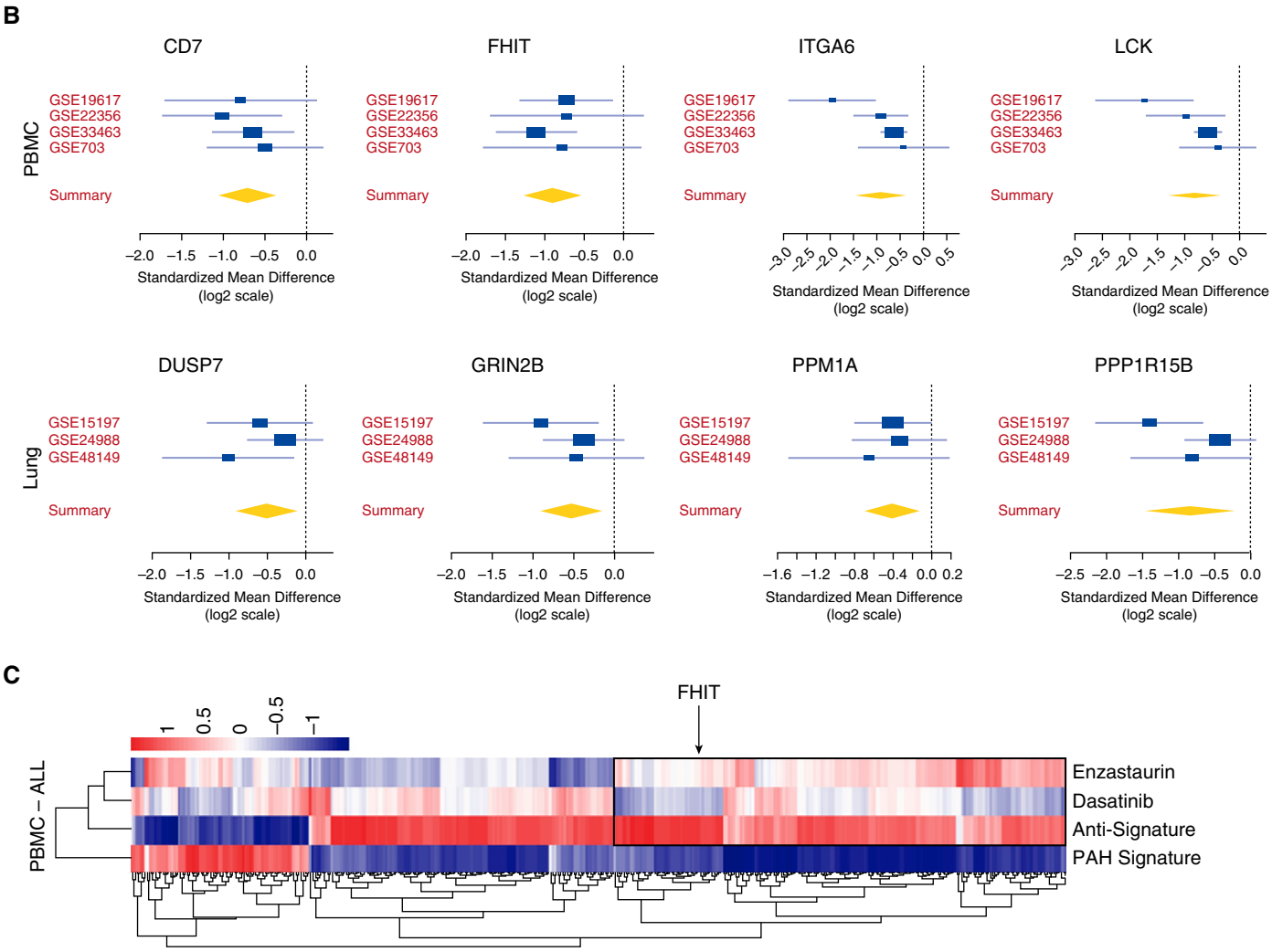

Figure 1. (Continued).

BMPR2 signaling. In a two-step screening approach, target gene siRNAs decreased Id1 expression to ⩽60%, comparable to siBMPR2, while maintaining a general cell viability of ⩾70% with four siRNAs or ⩾80% with two siRNAs, respectively, to exclude cell death response genes. This yielded 74 BMPR2-modifier gene candidates that were then compared with multicohort, multitissue PAH gene expression data sets obtained from the public domain (24–26) to identify a subset of genes that were differentially downregulated in patients with IPAH versus control subjects (Figure 1A). We identified eight candidate genes with decreased expression in patients with IPAH and thereby of potential clinical importance in PAH that overlapped with HTS candidate BMPR2-modifier genes: *ITGA6*, *FHIT*, *LCK* (lymphocyte-specific protein tyrosine kinase), and *CD7* from the PBMC data sets and *PP1R15B*, *PPM1A*, *GRIN2B*, and *DUSP7* from the lung datasets (Figure 1B). The most promising as related to PAH pathogenesis appeared to be *FHIT* and *LCK*. FHIT was most consistently reduced (by >50%), arguing for a consistent role in PAH pathology. LCK was strongly connected to PAH pathogenesis, as LCK is known to be inhibited by dasatinib (27), a reported trigger of drug-induced PAH (28).

We furthermore compared the PAH gene expression signature derived from the public available PAH transcriptomic PBMC data sets, predicted a complementary anti-PAH signature, and compared both with the gene expression profile of two drugs, dasatinib and enzastaurin, a drug known to increase FHIT. Both drug profiles were derived from the LINCS database that profiled a large number of drugs across many cell lines (www.lincscloud.org). In the gene cluster containing FHIT, enzastaurin-induced gene regulation was similar to the PAH antisignature (Figure 1C, box), whereas dasatinib-induced gene regulation resembled the PAH signature. We hypothesized that drugs that mimic the PAH gene expression signature may be detrimental to PAH, such as dasatinib, whereas drugs that reverse the PAH signature, such as enzastaurin, would be beneficial. As the list of enzastaurin-induced gene regulation shows, FHIT is one of many genes that is regulated by enzastaurin, supporting our findings of FHIT-independent enzastaurin drug effects.

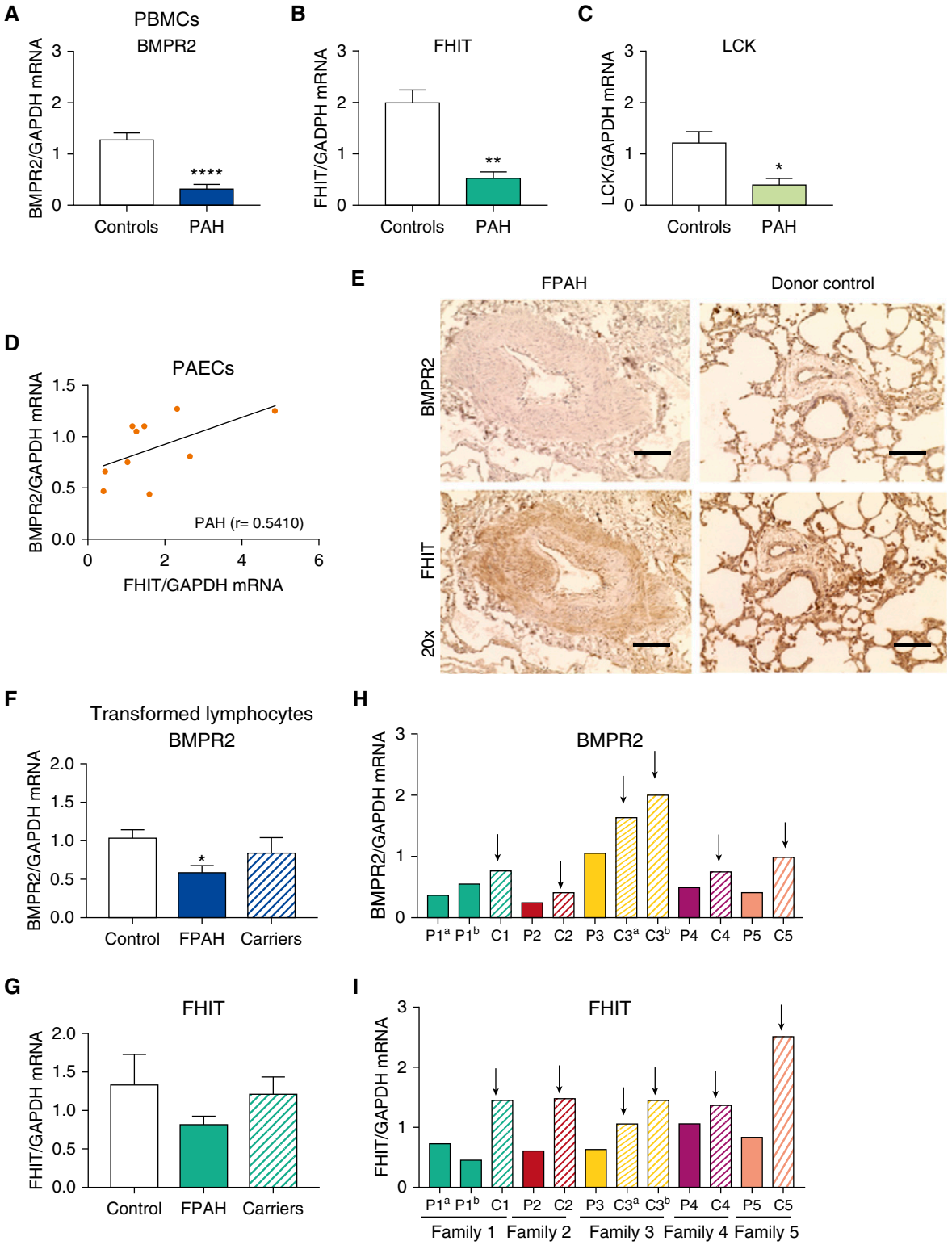

Figure 2. Attenuated FHIT (fragile histidine triad) expression in pulmonary arterial hypertension (PAH) correlates with decreased BMPR2 (bone morphogenetic protein receptor type 2) expression. (*A–C*) Quantitative PCR (qPCR) analysis of BMPR2 (*A*), FHIT (*B*), and LCK (lymphocyte-specific protein tyrosine kinase) (*C*) mRNA expression in peripheral blood mononuclear cells from patients with end-stage PAH with negative *BMPR2* mutation status compared with healthy control subjects (control, $n = 12$; PAH, $n = 8$; mean ± SEM; $^{*}P < 0.05$, $^{**}P < 0.01$, $^{****}P < 0.0001$ vs. control, Welch's *t* test). (*D*) Correlation and linear regression analysis of BMPR2 and FHIT mRNA expression in pulmonary artery endothelial cells from patients with idiopathic PAH (IPAH) at the time of lung transplant (control, $n = 6$; IPAH, $n = 6$; familial PAH [FPAH], $n = 4$; control, $r = -0.7714$; PAH, $r = 0.5410$; IPAH, $r = 0.5218$;

Downregulation of BMPR2 and Its Modifier Gene *FHIT* Is Observed in PAH Cells and Lung Tissue and Appears to Modify FPAH Disease Penetrance

As FHIT and LCK were identified in the PBMC gene expression data set, we first investigated whether FHIT was consistently decreased in cells from PAH patients, that is, PBMCs, PAECs, and transformed lymphocytes, as well as lung tissue.

We measured BMPR2, FHIT and LCK expression in PBMCs from eight patients with PAH without *BMPR2* mutations, and confirmed that expression of all three genes was significantly reduced (Figures 2A–2C). Microvascular ECs isolated from lungs from patients with IPAH harvested at the time of lung transplantation (12) (*see* Table E1 in the online supplement) showed a positive correlation between FHIT and BMPR2 mRNA expression (Figure 2D). Immunohistochemistry staining of FHIT and BMPR2 was reduced in patients with FPAH and IPAH compared with donor lungs (Figures 2E and E15 and Table E1). Although BMPR2 was strongly and uniformly reduced, as expected in the presence of a *BMPR2* mutation, the patchy decrease in FHIT was limited to the neointima and subendothelial layer (Figures 2E and E15), suggesting an incomplete overlap between FHIT and BMPR2 with regard to their gene expression and potential role in vascular remodeling.

We next determined the expression of these genes in patients with FPAH with a *BMPR2* mutation and healthy obligate BMPR2 carriers to assess whether they may modify disease penetrance in FPAH. A cohort of seven families with a *BMPR2* mutation was selected: 10 patients with a *BMPR2* mutation (P1–P8), 10 related healthy, obligate *BMPR2* mutation carriers (C1–C8), and unrelated healthy control subjects (Table E1). In transformed lymphocytes, extracted as previously described (29), BMPR2 and FHIT mRNA was consistently lower in patients than in healthy carriers (five of seven families), suggesting that FHIT may modify disease penetrance in *BMPR2* mutation carriers (Figures 2F–2I, E1G, and E1H). BMPR2 and FHIT levels were, however, variable among the families and different in males and females (Figures 2H, 2I, and E1), suggesting that the BMPR2 or FHIT threshold required to suppress PAH pathogenesis varies by genetic background and sex.

miR17-5 and miR27a Negatively Regulate FHIT/BMPR2 Signaling, Restored by Enzastaurin

We next identified that FHIT and LCK are upstream regulators of BMPR2. Knocking down FHIT and LCK in PAECs with siRNA decreased both the BMPR2 expression as well as its downstream signaling, measured by the target ID1 (Figures 3A and 3B). Conversely, siBMPR2 did not affect FHIT and LCK expression in PAECs, confirming that BMPR2 is downstream of FHIT and LCK (Figure 3C and 3D). Of interest, siFHIT decreased LCK expression to 50%, suggesting a potential interdependence of both modifier genes (Figure 3D).

How FHIT and LCK levels regulate BMPR2 expression is unknown. As microRNAs have been shown to play a major role in the regulation of BMPR2 signaling in PAH (30, 31), we used a candidate approach and investigated whether selected microRNAs would orchestrate FHIT- and LCK-mediated regulation of BMPR2 expression in PAECs. We focused on miR17-5 and miR100, both direct regulators of BMPR2, and miR27a, a readout for canonical Smad signaling (30, 32). Reductions of FHIT mRNA by siRNA increased the expression of miR17-5 (threefold to fourfold; Figures 3E and 3K) and miR27a (fourfold; Figure 3L), but not miR100 expression (Figure 3G). LCK deficiency strongly increased both miR17-5 and miR100 expression by eightfold or twofold, respectively (Figures 3E and 3F).

Treatment with enzastaurin for 24 hours (15 μM) increased FHIT, BMPR2, and Id1 expression in PAECs (Figures 3G–3I and E11). Interestingly, enzastaurin (15 μM) was able to rescue FHIT mRNA knockdown (treatment for 24 h after knockdown with siRNA, Figure 3J), supporting the previous finding that enzastaurin potently upregulates FHIT expression. Furthermore, enzastaurin inhibited siFHIT-mediated increases in miR17-5 and miR27a (Figures 3K and 3L), providing some mechanistic insight into how FHIT and enzastaurin might regulate BMPR2 levels by modulating miRNA expression (Figure 3M). We inhibited the siFHIT-mediated miR17-5 increase with concomitant anti–miR17-5 transfection and showed that blocking miR17-5 rescued BMPR2 and ID1 expression, suggesting that FHIT mediated BMPR2 modulation is in part miR17-5 dependent (Figure E10). We then determined whether the effect of enzastaurin on BMPR2 modulation is miR17-5 dependent and whether enzastaurin might even regulate FHIT via miR17-5 (Figure E16). In PAECs, enzastaurin downregulated miR17-5 and BMPR2 (Figures E16A and E16B). Adding an miR17-5 mimic to enzastaurin neutralized the effect of enzastaurin on miR17-5 as well as on BMPR2 expression, suggesting that the effect of enzastaurin on BMPR2 was miR17-5 dependent. Alternatively, the effect of enzastaurin on FHIT elevation was not miR17-5 dependent (Figure E16D), and also the effect of enzastaurin on Id1 did not require downregulation of miR17-5 (Figure E16C). We therefore concluded that enzastaurin can increase BMPR2 via a dual mechanism, that is, by reducing miR17-5 directly (independently of FHIT) and via increasing FHIT. Furthermore, the enzastaurin-mediated increase in Id1 expression was not miR17-5 dependent.

Enzastaurin Upregulates FHIT/BMPR2 Signaling and Prevents Vascular Dysfunction Induced by FHIT Deficiency *In Vitro*

Given that PAH is characterized by loss of pulmonary vessels (33), we investigated how FHIT expression relates to inhibition of vessel formation, increased apoptosis, DNA damage (34, 35), and cell

Figure 2. (Continued). Spearman *r*; for patient demographics, *see* Table E1B). (*E*) Representative pulmonary anti-BMPR2 and anti-FHIT immunohistochemistry (horseradish peroxidase, brown staining) in lung tissue from patients with PAH and donor control subjects at time of transplant ($n = 3$; for patient demographics, *see* Table E1C; scale bars, 20 μm). (*F* and *G*) qPCR analysis of FHIT and BMPR2 expression in transformed lymphocytes from patients with FPAH, nonaffected *BMPR2* mutation carriers, and healthy control subjects ($n = 10$; mean ± SEM; $^*P < 0.05$, one-way ANOVA, Dunnett *post hoc* test; for patient demographics, *see* Table E1A). (*H* and *I*) qPCR analysis of FHIT and BMPR2 expression in transformed lymphocytes from selected families ($n = 5$; P indicates patients with FPAH; C indicates healthy mutation carrier; the arrows point toward the carriers with consistently increased FHIT and BMPR2 compared with their FPAH family members; for patient demographics, *see* Table E1A). PAEC = pulmonary artery endothelial cell; PBMC = peripheral blood mononuclear cell.

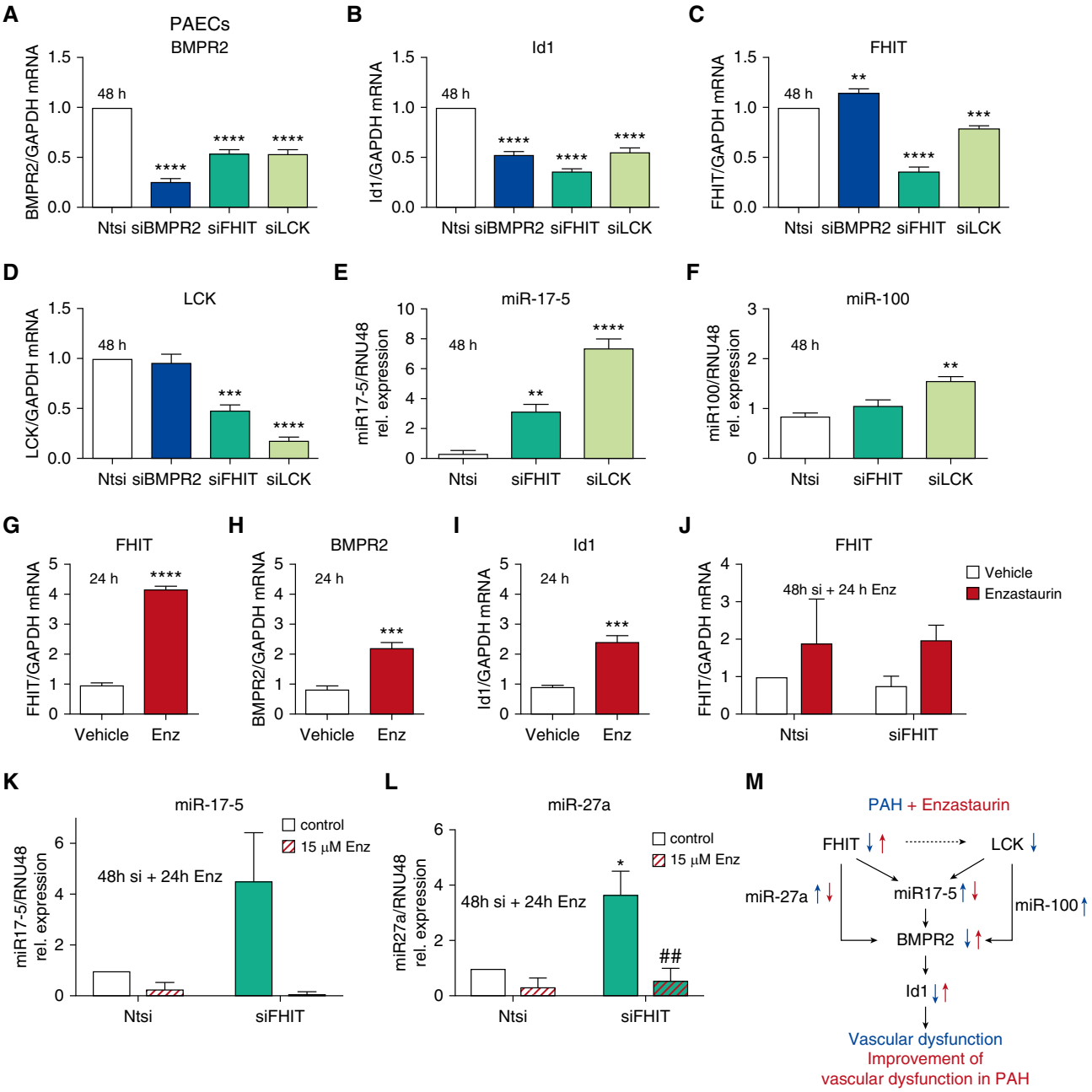

Figure 3. mRNA expression and microRNA profiling in siFHIT pulmonary artery endothelial cells (PAECs) reveals a potential role for microRNAs miR17-5 and miR27a in the regulation of BMPR2 (bone morphogenetic protein receptor type 2) signaling by FHIT that can be engaged by enzastaurin. (*A–D*) Relative mRNA expression of BMPR2 (*A*), Id1 (*B*), FHIT (*C*), and LCK (lymphocyte-specific protein tyrosine kinase) (*D*) normalized to GAPDH in PAECs transfected with an siBMPR2, siFHIT, siLCK, or nontargeting control (Ntsi) pool of four siRNAs (quantitative PCR [qPCR]; Amaxa Nucleofection, $t = 48$ h, $n = 3$, mean ± SEM; $^{**}P < 0.01$, $^{***}P < 0.001$, $^{****}P < 0.0001$ vs. control, one-way ANOVA, Tukey *post hoc* test). (*E* and *F*) Relative microRNA expression of miR17-5 (*E*) and miR100 (*F*) normalized to RNU48 in PAECs transfected with an siFHIT, siLCK, or nontargeting control pool of four siRNAs (qPCR; $t = 48$ h after transfection, $n = 3$, mean ± SEM; $^{**}P < 0.01$, $^{****}P < 0.0001$ vs. nontargeting control, one-way ANOVA; Dunnett *post hoc* test). (*G–I*) Relative mRNA expression of FHIT (*G*), BMPR2 (*H*), and Id1 (*I*) normalized to GAPDH in PAECs incubated with 15 μM enzastaurin for 24 hours (qPCR; $t =$ 72 h after transfection, $n = 3$, mean ± SEM; $^{***}P < 0.001$, $^{****}P < 0.0001$ vs. vehicle, unpaired *t* test). (*J*) Relative mRNA expression of FHIT normalized to GAPDH in PAECs transfected with an siFHIT or nontargeting control pool of four siRNAs, treated with or without 15 μM enzastaurin for 24 hours (qPCR; $t = 72$ h after transfection; RNAiMAX, $n = 4$; mean ± SEM). (*K* and *L*) Relative microRNA expression of miR17-5 (*K*) and miR27a (*L*) normalized to RNU48 in PAECs treated for 24 hours with or without 15 μM enzastaurin transfected with an siFHIT or nontargeting control pool of four siRNAs (qPCR; $t = 72$ h after transfection; $n = 3$; mean ± SEM; $^{*}P < 0.05$ vs. NTsi, $^{\#\#}P < 0.01$ vs. siFHIT control, two-way ANOVA, Dunnett *post hoc* test). (*M*) Schematic model of the proposed regulation of BMPR2 by FHIT. Enz = enzastaurin; FHIT = fragile histidine triad; PAH = pulmonary arterial hypertension.

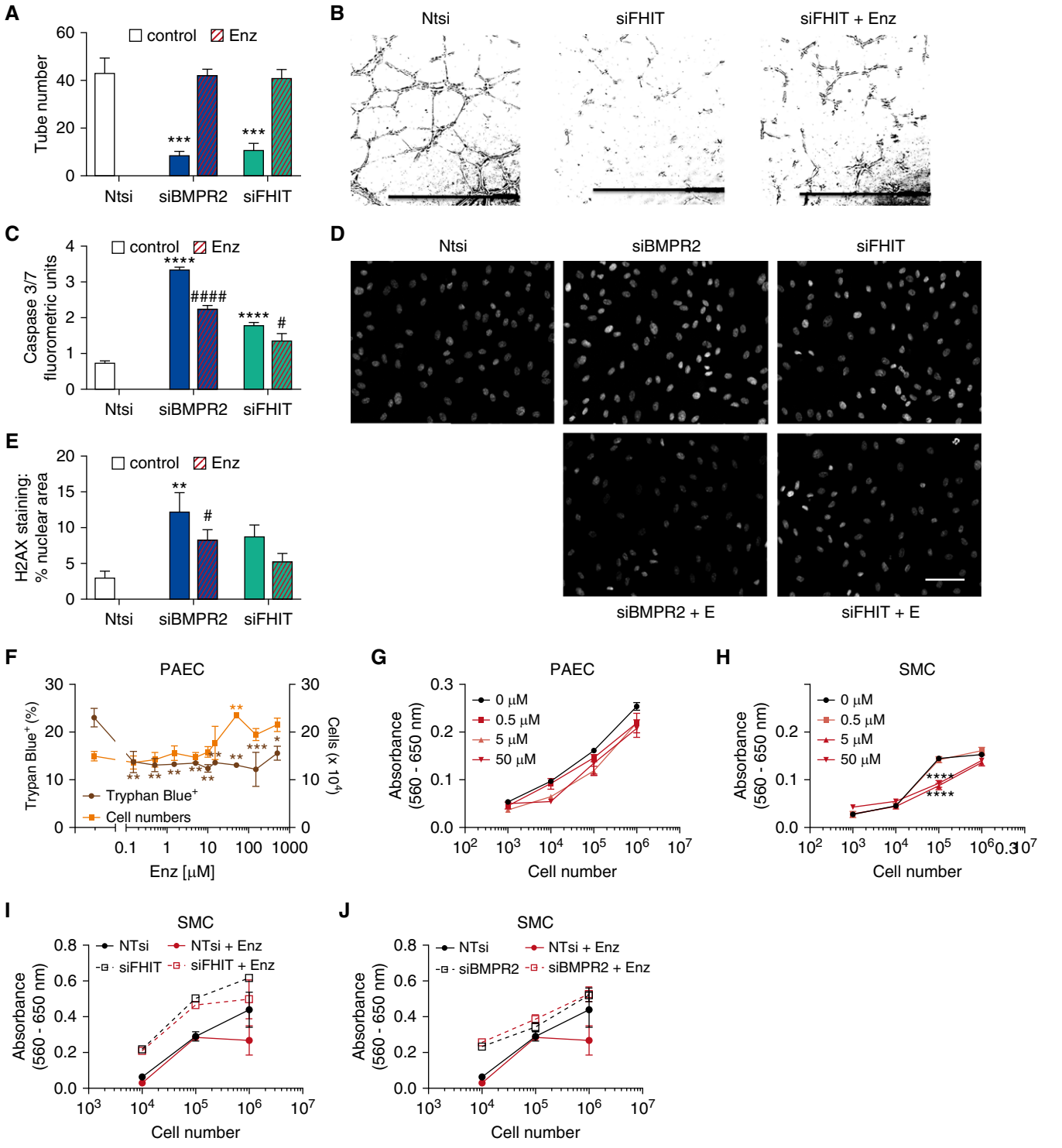

Figure 4. Enzastaurin increases expression of BMPR2 (bone morphogenetic protein receptor type 2) upstream signaling molecule FHIT (fragile histidine triad) in pulmonary artery endothelial cells (PAECs) and reverses pulmonary arterial hypertension–specific functional deficits in tube formation, apoptosis, DNA damage, and proliferation in FHIT-deficient PAECs. (*A* and *B*) Matrigel tube formation assay in siFHIT PAECs rescued by 15 μM enzastaurin for 24 hours ($t = 48$ h after transfection; Amaxa Nucleofection; nontargeting control [Ntsi], 43.3 ± 5.9; siBMPR2, 8.7 ± 1.5; siFHIT, 11.0 ± 2.6 tubes per average of five fields [20×]; $n = 3$; mean ± SEM; $^{***}P < 0.001$ vs. Ntsi, one-way ANOVA, Dunnett *post hoc* test; scale bars, 1 mm). (*C*) Caspase-3/7 luminescence in siBMPR2 and siFHIT PAECs rescued by 15 μM enzastaurin ($t = 48$ h after transfection; RNAiMAX, Caspase-Glo 3/7 assay; $n = 3$; mean ± SEM; $^{****}P < 0.0001$ vs. Ntsi, $^{\#}P < 0.05$, $^{\#\#\#\#}P < 0.0001$ vs. untreated control, one-way ANOVA, Dunnett *post hoc* test). (*D* and *E*) γH2AX staining in siBMPR2 and siFHIT PAECs rescued by 10 μM enzastaurin for 24 hours ($t = 72$ h after transfection; Dharmafect; $n = 3$; mean ± SEM;

proliferation in PAECs. We therefore assessed whether decreasing FHIT and BMPR2 expression in PAECs worsened EC dysfunction and whether treatment with enzastaurin for 24 hours could rescue the phenotype. Loss of FHIT and BMPR2 impaired PAECs tube formation 6 hours after cells were seeded in a Matrigel tube formation assay (12) compared with cells treated with control Ntsi (Figures 4A and 4B). Enzastaurin treatment fully reversed the defects in tube formation in FHIT- and BMPR2-deficient PAECs after 24 hours, in accordance with its ability to increase FHIT expression at this time point (Figure 3J).

As a cumulative viability measurement, we quantified caspase-3/7 activity, using the luminescent Caspase-Glo 3/7 assay (36), and DNA damage, using histone H2AX phosphorylation by immunofluorescence and quantification as nuclear area staining (percentage) by confocal microscopy (34, 35, 37). Reducing FHIT and BMPR2 mRNA activated caspases in PAECs 48 hours after transfection (Figure 4C), whereas enzastaurin decreased siBMPR2- and siFHIT-induced PAEC apoptosis. Reducing FHIT levels increased DNA damage after 48 hours about fourfold to Ntsi controls (Figures 4D and 4E), comparable to the degree of DNA damage observed in previous PBMC studies for patients with PAH (35). DNA damage induced by FHIT or BMPR2 loss was significantly attenuated by enzastaurin in PAECs. PAEC proliferation was assessed via a 3-[4,5-dimethylthiazol-2-yl]-2,5-diphenyltetrazolium bromide proliferation assay and hemocytometer cell counts (36). Enzastaurin did not elicit cell toxicity by a trypan blue viability assay. We rather observed increased cell numbers following treatment with enzastaurin (up to 50 μM), likely reflecting decreased apoptosis, as no increase in PAEC proliferation was detected (Figures 4F and 4G).

Given the role of SMCs in medial hypertrophy and vascular remodeling in PAH, we determined that reductions in FHIT (Figures 4H and 4I), but not BMPR2 (Figure 4J), increased PASMC proliferation *in vitro* (Figure 4I) that was rescued by enzastaurin. We conclude from these data that FHIT loss promotes PAEC and PASMC dysfunction, which can be improved by enzastaurin in an FHIT- and BMPR2-dependent manner. The stronger beneficial effect of enzastaurin on PAEC function compared with PASMC function might be explained by the stronger expression of BMPR2 in PAECs, which might make them more responsive to BMPR2-modulating therapies.

FHIT Deficiency *In Vivo* Predisposes to Exaggerated PH in Response to Hypoxia

Reduced FHIT in patients with PAH and the importance of adequate FHIT levels in EC and SMC function led us to determine whether FHIT loss predisposes to PH *in vivo*. $Fhit^{-/-}$ mice and wild-type littermates (8 wk of age, male/female) were exposed to chronic hypoxia (10%) for 3 weeks followed by a recovery period in normoxia (21%, 4 wk) (38, 39). PH was assessed by measurement of RV systolic pressure (RVSP) through the right jugular vein. Animals were killed and tissue was collected at 3 and 7 weeks, respectively. RV hypertrophy (RVH) was assayed using the weight ratio of the right ventricle to left ventricle and septum weight. C57BL/6 wild-type mice displayed a stereotypical adaptation response to hypoxia, with increases in RVSP (Figures 5A and E2), RVH (Figures 5B and E2), vascular rarefaction in arterioles and venules (Figures 5C and 5D), and increased muscularization (Figures 5E and 5F), all reversible upon return to room air. In contrast, $Fhit^{-/-}$ mice displayed an exaggerated increase in RVSP and RVH, increased vascular rarefaction, and muscularization in hypoxia, with incomplete resolution after 4 weeks of normoxia (Figures 5A–5F and E2) yet no RV fibrosis (Figure E9). Furthermore, baseline muscularization extended into more distal vessel generation in $Fhit^{-/-}$ mice (7–10 generations) compared with littermate control mice (Figures 5G and 5H), where no muscularized vessels were observed beyond the seventh generation (for detailed description, *see* online supplement) (40). Of note, we discovered a sex difference in the degree of baseline RVSP, RVH, vascular rarefaction and small vessel muscularization (for detailed description, *see* online supplement).

As expected, FHIT protein was absent in $Fhit^{-/-}$ lungs in all conditions (Figure 5I), and FHIT mRNA was not detectable in $Fhit^{-/-}$ lung tissue. The observed faint band on Western blot that runs slightly higher than FHIT is likely some unspecific band, as the $Fhit^{-/-}$ mouse contains a termination codon introduced into the exon 5 coding region of FHIT, with exon 5 being the first protein coding exon, so that the termination prevents translation of a protein (38, 41). Chronic hypoxia decreased BMPR2 protein in $Fhit^{-/-}$ lungs, correlating with the observed RVSP and RVH increases in chronic hypoxia in $Fhit^{-/-}$ mice (Figure 5I). Surprisingly, $Fhit^{-/-}$ mice exposed to hypoxia and treated with enzastaurin (5 mg/kg/d via mini-osmotic pump) showed an improved PH as well as increased BMPR2 and ID1 expression in whole-lung tissue, suggesting FHIT-independent mechanisms of enzastaurin on BMPR2 modulation (Figure E8). In line with our cell culture work, enzastaurin was able to decrease miR17-5 and miR27a, independent of FHIT (Figures E8F and E8G).

Enzastaurin Prevents PH in Mice Exposed to Chronic Hypoxia

Given the ability of enzastaurin to increase FHIT and BMPR2 levels as well as its beneficial effect on endothelial and smooth muscle cell dysfunction, we used enzastaurin in *in vivo* rodent models to assess its propensity to prevent or reverse experimental PH and vascular remodeling. Owing to the increased severity of PH in male $Fhit^{-/-}$ mice in hypoxia, we used enzastaurin exclusively in male animals. As

Figure 4. (Continued). $^{**}P < 0.01$ vs. Ntsi, $^{\#}P < 0.05$ vs. untreated control, one-way ANOVA, Dunnett *post hoc* test). The quantified area represents the percentage of cells that show nuclear γH2AX staining quantified with automated software (white nuclei show positive stain, gray nuclei show background stain). Scale bar, 50 μm. (*F*) Total cell counts and percentage trypan blue–positive PAECs cultured in varying concentrations of enzastaurin ($n = 3$; one-way ANOVA, $^{*}P < 0.05$, $^{**}P < 0.01$ vs. untreated control). (*G* and *H*) 3-[4,5-Dimethylthiazol-2-yl]-2,5-diphenyltetrazolium bromide (MTT) proliferation assay in enzastaurin-treated (0.5–50 μM) pulmonary arterial hypertension smooth muscle cells (PASMCs) and PAECs, respectively ($n = 3$). (*I* and *J*) MTT proliferation assay in enzastaurin-treated (5 μM) siFHIT- and siBMPR2-transfected PASMCs compared with Ntsi, respectively ($n = 3$). Enz = enzastaurin; SMC = smooth muscle cell.

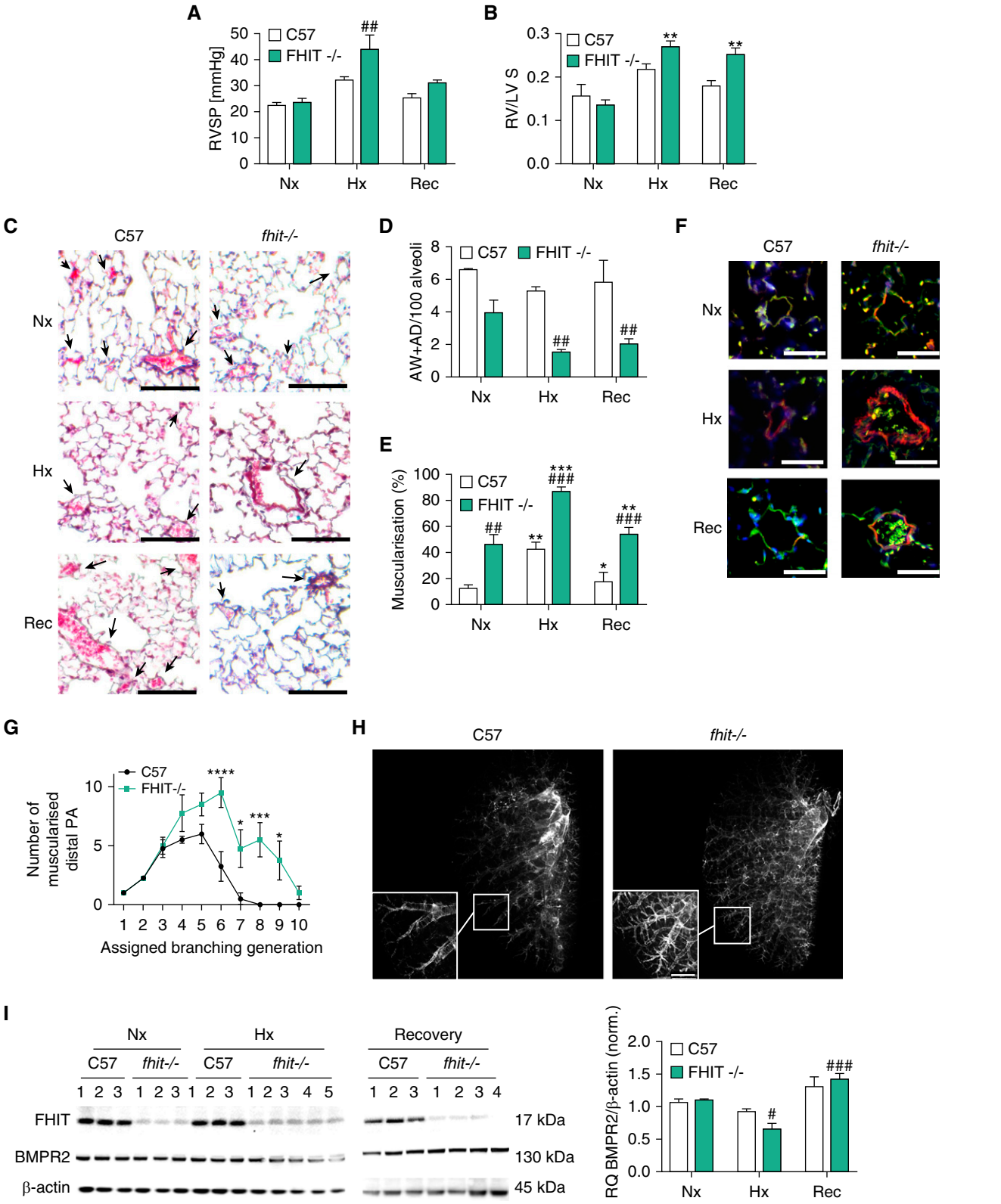

Figure 5. *Fhit*$^{-/-}$ C57BL/6 mice develop experimental pulmonary hypertension after chronic exposure to hypoxia. *Fhit*$^{-/-}$ C57BL/6 and littermate wild-type (C57) mice were housed for 3 weeks in normoxic (Nx, 21% O_2) and hypoxic (Hx, 10% O_2) conditions, with a hypoxia recovery (Rec, 3 wk Hx/4 wk Nx) period for 4 weeks, compared with 7 weeks for Nx control mice. (*A*) Right ventricular systolic pressure was measured by pulmonary artery catheterization (male, C57, $n = 3$; *Fhit*$^{-/-}$ Nx Rec, $n = 3$; *Fhit*$^{-/-}$ Hx, $n = 4$). (*B*) Right ventricular hypertrophy is demonstrated by the weight ratio of the right ventricle to left

a pilot prevention model, we exposed *Bmpr2*$^{+/-}$ mice and wild-type littermates (8 wk of age) to hypoxia (10%) for 3 weeks with a subcutaneously implanted mini-osmotic pump, supplying 15 mg/kg/d enzastaurin or vehicle. Enzastaurin prevented RVSP and RVH increases (Figure E4), vascular rarefaction, as well as muscularization of distal vessels (Figure E4) in *Bmpr2*$^{+/-}$ and wild-type mice. We furthermore treated C57BL6 mice exposed to 3 weeks of hypoxia with either FK506 (0.05 mg/kg/d), enzastaurin (5 mg/kg/d), or a combination of both and documented an additive effect of FK506 and enzastaurin with regard to prevention of PH (as measured by RVSP), BMPR2, as well as ID1 expression (Figure E7). The effect of enzastaurin in FHIT-competent animals seemed not solely to be mediated through miR-17-5 (Figure E7F) but potentially related to the effect of enzastaurin on miR27a (Figure E7G).

Enzastaurin Reverses Experimental PH in Sugen5416/Hypoxia/Normoxia Rats

As a reversal model, we used the Sugen5416/hypoxia/normoxia rat model, which mimics human end-stage PAH and is characterized by extensive vascular remodeling.

Sprague-Dawley rats were subcutaneously injected with 20 mg/kg Sugen5416 once and housed in chronic hypoxia (10%, 3 wk), followed by 5 weeks in normoxia as previously described (42). Eight weeks after subcutaneous Sugen5416 injection, rats received daily oral gavage with 5 mg/kg/d enzastaurin or vehicle control for 3 weeks. Hemodynamic assessment of the animals (echocardiography, right heart catheter) was performed before sacrifice and tissue collection. Rats developed severe obliterative end-stage PH that was characterized by luminal obliteration and right heart failure (Figuress 6D–6H and E5). Consistent with the histological observations, RVSP (>100 mm Hg) and RVH were severely increased in Sugen5416-injected rats (Figures 6A and 6B), and increased interstitial fibrosis was observed in the right ventricle in these animals (Figures 6I–6K).

Treatment with enzastaurin increased FHIT and BMPR2 expression in whole lungs (Figure 6G), nearly entirely reversed vascular occlusions (Figure 6D), and potently reduced muscularization of small and large vessels (Figure 6E), as well as RVH (Figure 6B) and RV fibrosis (Figure 6I). RVSP was reduced by >30 mm Hg in enzastaurin-treated Sugen5416/hypoxia/normoxia rats.

Discussion

BMPR2 signaling is severely impaired in patients with FPAH compared with unaffected mutation carriers (29, 43, 44), suggesting *1*) a threshold of BMPR2 expression or signaling below which PAH develops, *2*) the presence of BMPR2-modifying factors, or *3*) additional pathways that contribute to PAH pathogenesis.

We identified *FHIT* and *LCK* in an extensive siRNA HTS of >22,000 genes as novel BMPR2 modifier genes. To confirm a likely clinical importance in PAH, we cross-validated gene expression of both genes in a novel multicohort, multitissue analysis of PAH transcriptome databases that included all PAH etiologies and confirmed that FHIT was consistently and severely downregulated in all datasets. As downregulation of LCK was more variable, we mainly focused in this study on understanding the role of FHIT in PAH. FHIT was most consistently downregulated in PBMCs, which are thought to be valid surrogates for ubiquitous gene expression in patients with PAH (35, 43, 45–47). We validated our findings of reduced FHIT expression in human PAH lymphocytes, PAECs, and lung tissue, respectively.

We propose that *FHIT* is a modifier gene that contributes to variable penetrance of PAH in predisposed individuals with a *BMPR2* mutation, consistent with the multiple-hit theory of PAH development. In support of this proposal, the low penetrance of *BMPR2* mutations in PAH of 20% (1) is comparable to the genetic predisposition of mammary carcinoma by *BRCA1* mutations, with likewise only 20–45% penetrance (48). FHIT serves as a disease sensitizer in sporadic breast cancer, where a one allele loss of *BRCA1* and *FHIT* resulted in a poor prognosis with a more aggressive phenotype (48). Similarly, simultaneous loss of FHIT and p53 in lung cancer led to predisposition for aggressive lung cancer by dysregulating pro-proliferative pathways (49). Decreased FHIT was a prerequisite, but not sufficient, to induce a carcinogenous phenotype *in vitro* (50), consistent with the increased genomic instability in *Fhit*$^{-/-}$ mice (51).

We further propose that low FHIT levels might also contribute to the observed low levels of BMPR2 in patients without FPAH, given that we measured reduced FHIT expression across different PAH etiologies. The mechanism of reduced FHIT expression in PAH is unknown and warrants further investigation. Epigenetic silencing or heterozygous loss of *FHIT* may occur due to its location on the fragile site *FRA3B* (13), where strand breakages commonly appear following hypoxia or carcinogen exposure, such as cigarette smoke (52–54). Despite the reported independence of FHIT expression from *FRA3B* site breakage in healthy adults (55), the increased mutagen sensitivity and potential concomitant defects in the DNA damage repair system through p53 (56) may predispose patients with PAH to FHIT reductions. Alternatively, hypermethylation

Figure 5. (Continued). ventricle and septum weight (male, C57 Nx Rec, $n = 3$; C57 Hx, $n = 6$; *Fhit*$^{-/-}$ Nx Hx, $n = 3$; *Fhit*$^{-/-}$ Rec, $n = 4$). (*C*) Representative Movat lung histology. Arrows indicate vessel position. Scale bars, 200 μm. (*D*) Loss of alveolar wall (AW) and alveolar duct (AD) pulmonary vessels. (*E*) Full or partial muscularization (percentage) of AW or AD vessels was assessed in Movat-stained lung sections (male, C57, $n = 3$; *Fhit*$^{-/-}$ Nx, $n = 3$; *Fhit*$^{-/-}$ Hx Rec, $n = 4$). (*F*) Representative immunofluorescent microscopy of murine lungs stained with α smooth muscle actin (red), von Willebrand factor (green), and DAPI (blue). Scale bars, 20 μm. (*G* and *H*) Arterial muscularization in agarose-inflated lungs of normoxic wild-type and *Fhit*$^{-/-}$ mice was assessed by deep tissue imaging in arteries accompanying the left lobe secondary lateral airway branch L4 (L:L4) ($n = 4$, two-way ANOVA; for detailed description, *see* the METHODS section). Scale bar, 750 μm. (*I*) Representative immunoblots and relative densitometric analysis of FHIT and BMPR2 protein expression in lung tissue normalized to a β-actin housekeeping control (male, C57, $n = 3$; *Fhit*$^{-/-}$ Nx, $n = 3$; *Fhit*$^{-/-}$ Hx, $n = 5$; *Fhit*$^{-/-}$ Rec, $n = 4$). All bars denote mean ± SEM. In all panels, $^{*}P < 0.05$, $^{**}P < 0.01$, $^{***}P < 0.001$, $^{****}P < 0.0001$ versus C57 control; $^{\#}P < 0.05$, $^{\#\#}P < 0.01$, $^{\#\#\#}P < 0.001$ versus *FHIT*$^{-/-}$ control, two-way ANOVA, Tukey *post hoc* test. BMPR2 = bone morphogenetic protein receptor type 2; *Fhit* = fragile histidine triad; PA = pulmonary artery; RQ = relative quantity; RV/LV+S = weight ratio of the right ventricle to left ventricle and septum weight; RVSP = right ventricular systolic pressure.

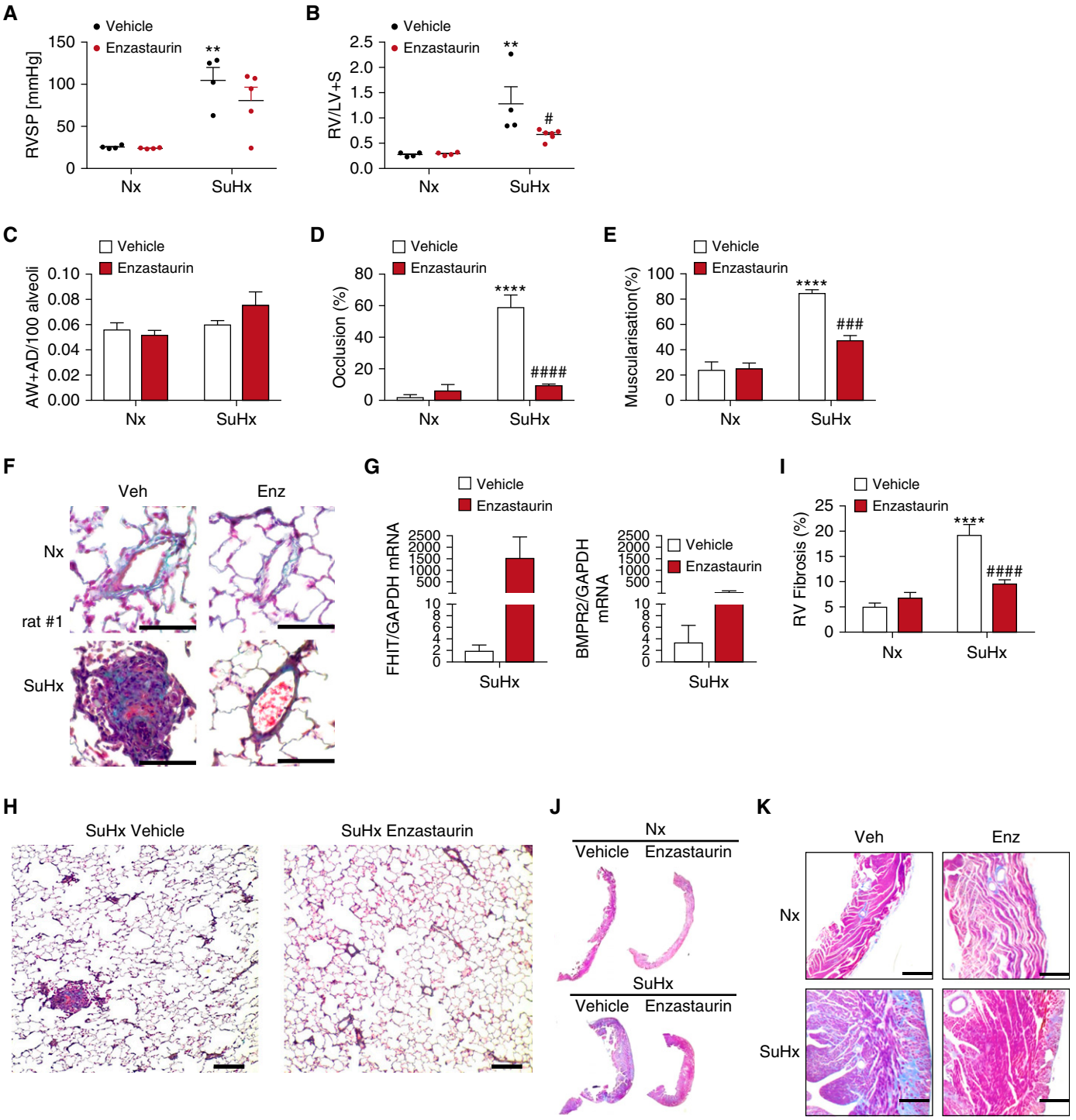

Figure 6. Enzastaurin reverses hemodynamic parameters, severe vascular remodeling, pulmonary emphysema, cardiac fibrosis, and right ventricular hypertrophy in Sugen5416/hypoxia rats. Experimental pulmonary hypertension was induced in male Sprague-Dawley rats by subcutaneous injection of 20 mg/kg body weight SU5416. Animals were housed for 3 weeks in hypoxic (Hx, 10% O_2) conditions, followed by a 5-week period in normoxia (Nx, 21% O_2), following daily administration of 5 mg/kg body weight enzastaurin or vehicle control by oral gavage. (*A*) Right ventricular systolic pressure was measured by pulmonary artery catheterization ($n = 4$; mean ± SEM; $^{**}P < 0.01$ vs. Nx control, one-way ANOVA, Sidak *post hoc* test). (*B*) Right ventricle hypertrophy is demonstrated by the weight ratio of the right ventricle to the left ventricle and septum ($n = 4$; mean ± SEM; $^{**}P < 0.01$ vs. Nx control, $^{\#}P < 0.05$ vs. vehicle control, two-way ANOVA, Tukey *post hoc* test). (*C*) Ratio of alveolar wall and alveolar duct pulmonary vessels, (*D*) their full or partial occlusion (percentage), and (*E*) their full or partial muscularization (percentage) were assessed in Movat-stained lung sections ($n = 4$; mean ± SEM; $^{****}P < 0.0001$ vs. Nx control, $^{\#\#\#}P < 0.001$, $^{\#\#\#\#}P < 0.0001$ vs. vehicle control, two-way ANOVA, Tukey *post hoc* test). (*F*) Representative Movat lung histology, highlighting large pulmonary vessels. Scale bars, 50 μm. (*G*) Relative mRNA expression of fragile histidine triad or bone morphogenetic protein receptor type 2 normalized to GAPDH in whole-lung tissue (quantitative PCR; $n = 4$;

of FHIT or its promoter (57–59) observed in malignancies such as lung cancer (60–64) may also account for low FHIT expression in PAH.

We confirmed that FHIT was an upstream regulator of BMPR2 and Id1 and that enzastaurin, a drug previously shown to increase FHIT expression (65), increased FHIT, BMPR2, and Id1 expression in PAECs. To mechanistically understand how FHIT might regulate BMPR2 signaling, we assessed the expression of selected BMPR2-regulatory microRNAs. Both miR17-5 and miR100 target BMPR2 in vascular (30, 66) and nonvascular cells alike (30, 66, 67). miR17-5 downregulates BMPR2 via IL-6/STAT3–mediated signaling (68). Reduced FHIT expression increases miR17-5, an effect rescued by enzastaurin. Reduced FHIT expression increases miR27a, an miRNA shown to be increased in PBMCs of patients with end-stage PAH (11). miR27a inhibition seems beneficial, as it reduced PAEC proliferation (30) and prevented PASMC growth in the pulmonary artery via BMPR2/PPARγ (69). Similar to miR17-5, enzastaurin was able to rescue the increase in miR27a induced by FHIT loss. Inhibiting miR17-5 using antagomirs rescued the siFHIT-induced BMPR2 repression, and might therefore present a promising treatment strategy, as similar approaches have recently shown (32, 70), with the caveat being that targeting single microRNAs likely represents too much of a reductionist approach to achieve significant improvement of vascular remodeling in human PAH.

Fhit$^{-/-}$ mice develop pulmonary hallmarks of PAH: muscularization of small arteries and distal artery rarefaction, exaggerated PH after hypoxia, as well as a failure to recover after reoxygenation. In that respect, *Fhit*$^{-/-}$ mice strongly resemble mice with an endothelial deletion of *Bmpr2* (71). In addition to absent FHIT expression throughout the experiment, *Fhit*$^{-/-}$ mice developed reduced BMPR2 levels in hypoxia compared with C57BL/6 mice, potentially accounting for the more severe PH phenotype in hypoxia. Whereas BMPR2 levels normalized after 4 weeks of reoxygenation, *Fhit*$^{-/-}$ mice still failed to fully recover, which could be explained either by a slower recovery from more severe vascular damage/dysfunction in *Fhit*$^{-/-}$ mice or additional BMPR2-independent roles of FHIT required for recovery. The finding that treatment with enzastaurin was able to improve PH in *Fhit*$^{-/-}$ mice and increase BMPR2 and ID1 expression was very surprising to us and suggests additional FHIT-independent effects of enzastaurin that are mediated by a direct regulation of miR17-5.

Vascular dysfunction in PAH is thought to be initiated by endothelial injury and early apoptosis leading to pulmonary vessel loss (12), followed by proliferation of apoptosis-resistant vascular cells (72). Heightened baseline DNA damage and mutagen sensitivity *in vivo* (26, 34, 35), which may predate disease onset (73), likely further contribute to EC vulnerability. FHIT loss leads to an increased sensitization to mutagen damage and therefore might pose a risk factor for vascular injury and failed recovery. We showed that reduced levels of FHIT and BMPR2 are associated with vascular dysfunction, causing apoptosis, impaired tube formation, and increased DNA damage in PAECs as well as heightened proliferation of PASMCs, consistent with the reported aggravation of DNA damage upon FHIT loss in preneoplasia (74). Alternatively, strategies that increase BMPR2 signaling, as we show in this study by using enzastaurin, improved these vascular phenotypes (7, 12, 75, 76).

FHIT is known to suppress EGFR/Src/ERK/Slug-regulated endothelial–mesenchymal transition in lung cancer cells. Reduced FHIT levels therefore could facilitate endothelial–mesenchymal transition, and, together with the increased proliferation of SMCs with low FHIT levels, could explain the increase in α smooth muscle actin–positive cells, medial hypertrophy, and adventitial hypertrophy of distal pulmonary vessels that we have observed (77–79). The vascular rarefaction observed in *Fhit*$^{-/-}$ mice may be attributed to increased PAEC apoptosis in distal arteries, defects in cell–cell adhesion, or migration of PAECs to sites of vascular injury, as evidenced by increased numbers of circulating ECs in patients with PAH (80).

As a proof of concept for the potential use of enzastaurin in BMPR2-deficient patients with PAH, we first investigated enzastaurin in *Bmpr2*$^{+/-}$ and wild-type C57BL/6 mice and provided evidence that a 2-week treatment with enzastaurin (15 mg/kg/d) attenuated hypoxia-induced PH, as measured by changes in RVSP, RVH, and pulmonary physiology. For potential translational relevance, we found an additive effect of FK506 and enzastaurin treatment in mice (Figure E4).

We then set out to test enzastaurin in the Sugen5416/hypoxia/normoxia rat model that develops severe pulmonary vascular remodeling that most closely mimics the human disease (42), including the severe neointima formation and RV failure (81), thus being superior to mouse models and the monocrotaline rat model that develops severe PH predominantly due to medial hypertrophy (82). Few studies have demonstrated reversal of established PH in Sugen5416/hypoxia/normoxia rats (6, 12, 32, 83, 84). We found that low-dose enzastaurin (5 mg/kg/d) potently reversed Sugen5416/hypoxia/normoxia-induced lung and RV damage by increasing FHIT and BMPR2 signaling. The interpretation of the finding is limited, which is based on the small sample size. Although enzastaurin is evaluated as a PKCβ inhibitor in cancer (21), we did not observe a significant decrease in PKC activation as measured by its phosphorylation (Figure E6) in whole-lung tissue after enzastaurin treatment of Sugen5416/hypoxia/normoxia-treated rats. We confirmed that enzastaurin increased FHIT and BMPR2 at low doses (5–15 μM) *in vitro* (Figure E12) and that enzastaurin differs from other selective PKCβ and global PKC inhibitors with regard to its potential to modulate FHIT, BMPR2, and ID as well as is effect on PAEC function (Figures E13 and E14). This might be due to our relative low-dose enzastaurin treatment *in vivo* compared with previous

Figure 6. (Continued). mean ± SEM; two-way ANOVA). (*H*) Representative Movat lung histology, presenting vessel occlusion (scale bars, 200 μm). (*I*) Percentage of fibrotic tissue compared with total tissue in the right ventricle ($n = 4$; mean ± SEM; $^{****}P < 0.0001$ vs. Nx control, $^{\#\#\#\#}P < 0.0001$ vs. vehicle control, two-way ANOVA, Tukey *post hoc* test). (*J* and *K*) Representative trichrome stains of whole right ventricle histology (*J*) and magnified sections (*K*) are displayed (scale bars, 200 μm). AD = alveolar duct; AW = alveolar wall; BMPR2 = bone morphogenetic protein receptor type 2; Enz = enzastaurin; FHIT = fragile histidine triad; RV = right ventricle; RV/LV+S = weight ratio of the right ventricle to left ventricle and septum weight; RVSP = right ventricular systolic pressure.

clinical trials (85, 86) and in *in vivo* rodent studies (87) and doses required to achieve reductions in protein kinase C phosphorylation *in vitro* (88). Efficacy in our rodent models was seen at doses corresponding to human equivalent doses of 0.8–1.4 mg/kg/d, substantially lower than the 4–17 mg/kg/d doses used in oncology trials, species-specific differences notwithstanding (89). We therefore propose that the effect of enzastaurin on vascular remodeling as well as FHIT expression that we observed is largely protein kinase C–independent. How enzastaurin increases FHIT is unknown; however, one potential mechanism may be Scr-mediated inhibition of FHIT phosphorylation and prevention of its subsequent degradation (90, 91).

Conclusions

We are proposing a novel role of FHIT in PAH pathogenesis as a BMPR2 modifier gene, providing insight into BMPR2 regulation as well as opportunities for PAH intervention. FHIT expression is consistently downregulated in PAH. Reduced FHIT levels reduce BMPR2 expression and signaling, and FHIT loss *in vivo* leads to exaggerated experimental PH in response to hypoxia. FHIT expression can be readily increased by enzastaurin, which was beneficial in the prevention and treatment of experimental PH in *Bmpr2*$^{+/-}$ mice and Sugen5416/hypoxia/normoxia rats. As enzastaurin also exhibits FHIT-independent effects mediated via miR17-5, it is difficult to exactly determine to what extent enzastaurin reverses PH via FHIT modulation. We conclude that FHIT is a novel and potentially essential component of the BMPR2 signaling architecture in PAH and that reduced FHIT levels can predispose to PAH development. Our studies support the further exploration of enzastaurin as a potentially beneficial treatment for PAH. ■

Author disclosures are available with the text of this article at www.atsjournals.org.

Acknowledgement: The authors thank the Pulmonary Hypertension Breakthrough Initiative for assistance in our study by providing patient samples.

References

1. Austin ED, Loyd JE, Phillips JA III. Heritable pulmonary arterial hypertension. 2002 Jul 18 [updated 2015 Jun 11; accessed 2018 Jun]. In: Adam MP, Ardinger HH, Pagon RA, Wallace SE, Bean LJH, Stephens K, *et al.*, editors. GeneReviews. Seattle, WA: University of Washington, Seattle; 1993–2018. Available from: https://www.ncbi.nlm.nih.gov/books/NBK1485/.
2. Lane KB, Machado RD, Pauciulo MW, Thomson JR, Phillips JA III, Loyd JE, *et al*.; International PPH Consortium. Heterozygous germline mutations in *BMPR2*, encoding a TGF-β receptor, cause familial primary pulmonary hypertension. *Nat Genet* 2000;26:81–84.
3. Fessel JP, Loyd JE, Austin ED. The genetics of pulmonary arterial hypertension in the post-*BMPR2* era. *Pulm Circ* 2011;1:305–319.
4. Atkinson C, Stewart S, Upton PD, Machado R, Thomson JR, Trembath RC, *et al*. Primary pulmonary hypertension is associated with reduced pulmonary vascular expression of type II bone morphogenetic protein receptor. *Circulation* 2002;105:1672–1678.
5. Rich JD, Shah SJ, Swamy RS, Kamp A, Rich S. Inaccuracy of Doppler echocardiographic estimates of pulmonary artery pressures in patients with pulmonary hypertension: implications for clinical practice. *Chest* 2011;139:988–993.
6. Long L, Ormiston ML, Yang X, Southwood M, Gräf S, Machado RD, *et al*. Selective enhancement of endothelial BMPR-II with BMP9 reverses pulmonary arterial hypertension. *Nat Med* 2015;21:777–785.
7. Long L, Yang X, Southwood M, Lu J, Marciniak SJ, Dunmore BJ, *et al*. Chloroquine prevents progression of experimental pulmonary hypertension via inhibition of autophagy and lysosomal bone morphogenetic protein type II receptor degradation. *Circ Res* 2013;112:1159–1170.
8. Brittain EL, Thennapan T, Maron BA, Chan SY, Austin ED, Spiekerkoetter E, *et al*. Update in pulmonary vascular disease 2016 and 2017. *Am J Respir Crit Care Med* 2018;198:13–23.
9. Liu D, Yan Y, Chen JW, Yuan P, Wang XJ, Jiang R, *et al*. Hypermethylation of *BMPR2* promoter occurs in patients with heritable pulmonary arterial hypertension and inhibits *BMPR2* expression. *Am J Respir Crit Care Med* 2017;196:925–928.
10. Spiekerkoetter E, Sung YK, Sudheendra D, Scott V, Del Rosario P, Bill M, *et al*. Randomised placebo-controlled safety and tolerability trial of FK506 (tacrolimus) for pulmonary arterial hypertension. *Eur Respir J* 2017;50:1602449.
11. Spiekerkoetter E, Sung YK, Sudheendra D, Bill M, Aldred MA, van de Veerdonk MC, *et al*. Low-dose FK506 (tacrolimus) in end-stage pulmonary arterial hypertension. *Am J Respir Crit Care Med* 2015;192:254–257.
12. Spiekerkoetter E, Tian X, Cai J, Hopper RK, Sudheendra D, Li CG, *et al*. FK506 activates BMPR2, rescues endothelial dysfunction, and reverses pulmonary hypertension. *J Clin Invest* 2013;123:3600–3613.
13. Huebner K, Garrison PN, Barnes LD, Croce CM. The role of the *FHIT/FRA3B* locus in cancer. *Annu Rev Genet* 1998;32:7–31.
14. Sozzi G, Sard L, De Gregorio L, Marchetti A, Musso K, Buttitta F, *et al*. Association between cigarette smoking and *FHIT* gene alterations in lung cancer. *Cancer Res* 1997;57:2121–2123.
15. Thavathiru E, Ludes-Meyers JH, MacLeod MC, Aldaz CM. Expression of common chromosomal fragile site genes, WWOX/FRA16D and FHIT/FRA3B is downregulated by exposure to environmental carcinogens, UV, and BPDE but not by IR. *Mol Carcinog* 2005;44:174–182.
16. Kujan O, Abuderman A, Al-Shawaf AZ. Immunohistochemical characterization of FHIT expression in normal human tissues. *Interv Med Appl Sci* 2016;8:7–13.
17. Sozzi G, Pastorino U, Moiraghi L, Tagliabue E, Pezzella F, Ghirelli C, *et al*. Loss of *FHIT* function in lung cancer and preinvasive bronchial lesions. *Cancer Res* 1998;58:5032–5037.
18. Campiglio M, Pekarsky Y, Menard S, Tagliabue E, Pilotti S, Croce CM. *FHIT* loss of function in human primary breast cancer correlates with advanced stage of the disease. *Cancer Res* 1999;59:3866–3869.
19. Toledo G, Sola JJ, Lozano MD, Soria E, Pardo J. Loss of FHIT protein expression is related to high proliferation, low apoptosis and worse prognosis in non-small-cell lung cancer. *Mod Pathol* 2004;17:440–448.
20. Huang Q, Liu Z, Xie F, Liu C, Shao F, Zhu CL, Hu S. Fragile histidine triad (FHIT) suppresses proliferation and promotes apoptosis in cholangiocarcinoma cells by blocking PI3K-Akt pathway. ScientificWorldJournal. 2014;2014:179698.
21. Robertson MJ, Kahl BS, Vose JM, de Vos S, Laughlin M, Flynn PJ, *et al*. Phase II study of enzastaurin, a protein kinase C beta inhibitor, in patients with relapsed or refractory diffuse large B-cell lymphoma. *J Clin Oncol* 2007;25:1741–1746.
22. Dannewitz Prosseda S, Suheendra D, Tian X, Kung J, Bohm M, Kumamoto K, *et al*. Enzastaurin reverses pulmonary arterial hypertension by targeting the novel BMPR2 modifier FHIT [abstract]. *Am J Respir Crit Care Med* 2017;195:A4228.
23. Austin ED, Hamid R, Hemnes AR, Loyd JE, Blackwell T, Yu C, *et al*. BMPR2 expression is suppressed by signaling through the estrogen receptor. *Biol Sex Differ* 2012;3:6.
24. Khatri P, Roedder S, Kimura N, De Vusser K, Morgan AA, Gong Y, *et al*. A common rejection module (CRM) for acute rejection across multiple organs identifies novel therapeutics for organ transplantation. *J Exp Med* 2013;210:2205–2221.

25. Sweeney TE, Haynes WA, Vallania F, Ioannidis JP, Khatri P. Methods to increase reproducibility in differential gene expression via meta-analysis. *Nucleic Acids Res* 2017;45:e1.
26. Li MD, Burns TC, Morgan AA, Khatri P. Integrated multi-cohort transcriptional meta-analysis of neurodegenerative diseases. *Acta Neuropathol Commun* 2014;2:93.
27. Lee KC, Ouwehand I, Giannini AL, Thomas NS, Dibb NJ, Bijlmakers MJ. Lck is a key target of imatinib and dasatinib in T-cell activation. *Leukemia* 2010;24:896–900.
28. Montani D, Bergot E, Günther S, Savale L, Bergeron A, Bourdin A, *et al*. Pulmonary arterial hypertension in patients treated by dasatinib. *Circulation* 2012;125:2128–2137.
29. Hamid R, Cogan JD, Hedges LK, Austin E, Phillips JA III, Newman JH, *et al*. Penetrance of pulmonary arterial hypertension is modulated by the expression of normal *BMPR2* allele. *Hum Mutat* 2009;30: 649–654.
30. Drake KM, Zygmunt D, Mavrakis L, Harbor P, Wang L, Comhair SA, *et al*. Altered microRNA processing in heritable pulmonary arterial hypertension: an important role for Smad-8. *Am J Respir Crit Care Med* 2011;184:1400–1408.
31. Caruso P, MacLean MR, Khanin R, McClure J, Soon E, Southgate M, *et al*. Dynamic changes in lung microRNA profiles during the development of pulmonary hypertension due to chronic hypoxia and monocrotaline. *Arterioscler Thromb Vasc Biol* 2010;30:716–723.
32. Thompson AAR, Lawrie A. Targeting vascular remodeling to treat pulmonary arterial hypertension. *Trends Mol Med* 2017;23:31–45.
33. Hislop A, Reid L. New findings in pulmonary arteries of rats with hypoxia-induced pulmonary hypertension. *Br J Exp Pathol* 1976;57: 542–554.
34. Meloche J, Pflieger A, Vaillancourt M, Paulin R, Potus F, Zervopoulos S, *et al*. Role for DNA damage signaling in pulmonary arterial hypertension. *Circulation* 2014;129:786–797.
35. Federici C, Drake KM, Rigelsky CM, McNelly LN, Meade SL, Comhair SA, *et al*. Increased mutagen sensitivity and DNA damage in pulmonary arterial hypertension. *Am J Respir Crit Care Med* 2015;192:219–228.
36. de Jesus Perez VA, Alastalo TP, Wu JC, Axelrod JD, Cooke JP, Amieva M, *et al*. Bone morphogenetic protein 2 induces pulmonary angiogenesis via Wnt–β-catenin and Wnt–RhoA–Rac1 pathways. *J Cell Biol* 2009;184:83–99.
37. Chen PI, Cao A, Miyagawa K, Tojais NF, Hennigs JK, Li CG, *et al*. Amphetamines promote mitochondrial dysfunction and DNA damage in pulmonary hypertension. *JCI Insight* 2017;2:e90427.
38. Fong LY, Fidanza V, Zanesi N, Lock LF, Siracusa LD, Mancini R, *et al*. Muir–Torre-like syndrome in Fhit-deficient mice. *Proc Natl Acad Sci USA* 2000;97:4742–4747.
39. Zanesi N, Fidanza V, Fong LY, Mancini R, Druck T, Valtieri M, *et al*. The tumor spectrum in *FHIT*-deficient mice. *Proc Natl Acad Sci USA* 2001;98:10250–10255.
40. Metzger RJ, Klein OD, Martin GR, Krasnow MA. The branching programme of mouse lung development. *Nature* 2008;453:745–750.
41. Pekarsky Y, Druck T, Cotticelli MG, Ohta M, Shou J, Mendrola J, *et al*. The murine *Fhit* locus: isolation, characterization, and expression in normal and tumor cells. *Cancer Res* 1998;58:3401–3408.
42. Abe K, Toba M, Alzoubi A, Ito M, Fagan KA, Cool CD, *et al*. Formation of plexiform lesions in experimental severe pulmonary arterial hypertension. *Circulation* 2010;121:2747–2754.
43. Meyrick BO, Friedman DB, Billheimer DD, Cogan JD, Prince MA, Phillips JA III, *et al*. Proteomics of transformed lymphocytes from a family with familial pulmonary arterial hypertension. *Am J Respir Crit Care Med* 2008;177:99–107.
44. Gu M, Shao NY, Sa S, Li D, Termglinchan V, Ameen M, *et al*. Patient-specific iPSC-derived endothelial cells uncover pathways that protect against pulmonary hypertension in BMPR2 mutation carriers. *Cell Stem Cell* 2017;20:490–504.e5.
45. Nicolls MR, Taraseviciene-Stewart L, Rai PR, Badesch DB, Voelkel NF. Autoimmunity and pulmonary hypertension: a perspective. *Eur Respir J* 2005;26:1110–1118.
46. Rabinovitch M, Guignabert C, Humbert M, Nicolls MR. Inflammation and immunity in the pathogenesis of pulmonary arterial hypertension. *Circ Res* 2014;115:165–175.
47. Hemnes AR, Trammell AW, Archer SL, Rich S, Yu C, Nian H, *et al*. Peripheral blood signature of vasodilator-responsive pulmonary arterial hypertension. *Circulation* 2015;131:401–409, discussion 409.
48. Silva Soares EW, de Lima Santos SC, Bueno AG, Cavalli IJ, Cavalli LR, Fouto Matias JE, *et al*. Concomitant loss of heterozygosity at the *BRCA1* and *FHIT* genes as a prognostic factor in sporadic breast cancer. *Cancer Genet Cytogenet* 2010;199:24–30.
49. Andriani F, Roz E, Caserini R, Conte D, Pastorino U, Sozzi G, *et al*. Inactivation of both FHIT and p53 cooperate in deregulating proliferation-related pathways in lung cancer. *J Thorac Oncol* 2012; 7:631–642.
50. Pekarsky Y, Zanesi N, Palamarchuk A, Huebner K, Croce CM. FHIT: from gene discovery to cancer treatment and prevention. *Lancet Oncol* 2002;3:748–754.
51. Paisie CA, Schrock MS, Karras JR, Zhang J, Miuma S, Ouda IM, *et al*. Exome-wide single-base substitutions in tissues and derived cell lines of the constitutive Fhit knockout mouse. *Cancer Sci* 2016;107: 528–535.
52. Schiess R, Senn O, Fischler M, Huber LC, Vatandaslar S, Speich R, *et al*. Tobacco smoke: a risk factor for pulmonary arterial hypertension? A case-control study. *Chest* 2010;138:1086–1092.
53. Huebner K, Croce CM. *FRA3B* and other common fragile sites: the weakest links. *Nat Rev Cancer* 2001;1:214–221.
54. Yoo YG, Christensen J, Huang LE. HIF-1α confers aggressive malignant traits on human tumor cells independent of its canonical transcriptional function. *Cancer Res* 2011;71:1244–1252.
55. Michael D, Rajewsky MF. Induction of the common fragile site FRA3B does not affect *FHIT* expression. *Oncogene* 2001;20: 1798–1801.
56. Jacquin S, Rincheval V, Mignotte B, Richard S, Humbert M, Mercier O, *et al*. Inactivation of p53 is sufficient to induce development of pulmonary hypertension in rats. *PLoS One* 2015; 10:e0131940.
57. Yan W, Xu N, Han X, Zhou XM, He B. The clinicopathological significance of FHIT hypermethylation in non-small cell lung cancer, a meta-analysis and literature review. *Sci Rep* 2016;6:19303.
58. Wali A. FHIT: doubts are clear now. *Sci World J* 2010;10:1142–1151.
59. Guler G, Iliopoulos D, Han SY, Fong LY, Lubet RA, Grubbs CJ, *et al*. Hypermethylation patterns in the *Fhit* regulatory region are tissue specific. *Mol Carcinog* 2005;43:175–181.
60. Tanaka H, Shimada Y, Harada H, Shinoda M, Hatooka S, Imamura M, *et al*. Methylation of the 5′ CpG island of the *FHIT* gene is closely associated with transcriptional inactivation in esophageal squamous cell carcinomas. *Cancer Res* 1998;58:3429–3434.
61. Zöchbauer-Müller S, Fong KM, Maitra A, Lam S, Geradts J, Ashfaq R, *et al*. 5′ CpG island methylation of the FHIT gene is correlated with loss of gene expression in lung and breast cancer. *Cancer Res* 2001; 61:3581–3585.
62. Yang Q, Nakamura M, Nakamura Y, Yoshimura G, Suzuma T, Umemura T, *et al*. Two-hit inactivation of *FHIT* by loss of heterozygosity and hypermethylation in breast cancer. *Clin Cancer Res* 2002;8: 2890–2893.
63. Dhillon VS, Shahid M, Husain SA. *CpG* methylation of the *FHIT*, *FANCF*, *cyclin-D2*, *BRCA2* and *RUNX3* genes in granulosa cell tumors (*GCTs*) of ovarian origin. *Mol Cancer* 2004;3:33.
64. Kim JS, Kim H, Shim YM, Han J, Park J, Kim DH. Aberrant methylation of the *FHIT* gene in chronic smokers with early stage squamous cell carcinoma of the lung. *Carcinogenesis* 2004;25: 2165–2171.
65. Körner A, Mudduluru G, Manegold C, Allgayer H. Enzastaurin inhibits invasion and metastasis in lung cancer by diverse molecules. *Br J Cancer* 2010;103:802–811.
66. Zeng Y, Qu X, Li H, Huang S, Wang S, Xu Q, *et al*. MicroRNA-100 regulates osteogenic differentiation of human adipose-derived mesenchymal stem cells by targeting BMPR2. *FEBS Lett* 2012;586: 2375–2381.
67. Sun Q, Mao S, Li H, Zen K, Zhang CY, Li L. Role of miR-17 family in the negative feedback loop of bone morphogenetic protein signaling in neuron. *PLoS One* 2013;8:e83067.

68. Brock M, Trenkmann M, Gay RE, Michel BA, Gay S, Fischler M, *et al*. Interleukin-6 modulates the expression of the bone morphogenic protein receptor type II through a novel STAT3–microRNA cluster 17/92 pathway. *Circ Res* 2009;104:1184–1191.
69. Hansmann G, de Jesus Perez VA, Alastalo TP, Alvira CM, Guignabert C, Bekker JM, *et al*. An antiproliferative BMP-2/PPARγ/apoE axis in human and murine SMCs and its role in pulmonary hypertension. *J Clin Invest* 2008;118:1846–1857.
70. Brock M, Samillan VJ, Trenkmann M, Schwarzwald C, Ulrich S, Gay RE, *et al*. AntagomiR directed against miR-20a restores functional BMPR2 signalling and prevents vascular remodelling in hypoxia-induced pulmonary hypertension. *Eur Heart J* 2014;35:3203–3211.
71. Diebold I, Hennigs JK, Miyagawa K, Li CG, Nickel NP, Kaschwich M, *et al*. BMPR2 preserves mitochondrial function and DNA during reoxygenation to promote endothelial cell survival and reverse pulmonary hypertension. *Cell Metab* 2015;21:596–608.
72. Rabinovitch M. Molecular pathogenesis of pulmonary arterial hypertension. *J Clin Invest* 2012;122:4306–4313.
73. Aldred MA, Comhair SA, Varella-Garcia M, Asosingh K, Xu W, Noon GP, *et al*. Somatic chromosome abnormalities in the lungs of patients with pulmonary arterial hypertension. *Am J Respir Crit Care Med* 2010;182: 1153–1160.
74. Cirombella R, Montrone G, Stoppacciaro A, Giglio S, Volinia S, Graziano P, *et al*. Fhit loss in lung preneoplasia: relation to DNA damage response checkpoint activation. *Cancer Lett* 2010;291: 230–236.
75. Drake KM, Dunmore BJ, McNelly LN, Morrell NW, Aldred MA. Correction of nonsense *BMPR2* and *SMAD9* mutations by ataluren in pulmonary arterial hypertension. *Am J Respir Cell Mol Biol* 2013;49:403–409.
76. Betapudi V, Shukla M, Alluri R, Merkulov S, McCrae KR. Novel role for p56/Lck in regulation of endothelial cell survival and angiogenesis. *FASEB J* 2016;30:3515–3526.
77. Joannes A, Grelet S, Duca L, Gilles C, Kileztky C, Dalstein V, *et al*. Fhit regulates EMT targets through an EGFR/Src/ERK/Slug signaling axis in human bronchial cells. *Mol Cancer Res* 2014;12:775–783.
78. Joannes A, Bonnomet A, Bindels S, Polette M, Gilles C, Burlet H, *et al*. Fhit regulates invasion of lung tumor cells. *Oncogene* 2010;29:1203–1213.
79. Suh SS, Yoo JY, Cui R, Kaur B, Huebner K, Lee TK, *et al*. FHIT suppresses epithelial-mesenchymal transition (EMT) and metastasis in lung cancer through modulation of microRNAs. *PLoS Genet* 2014; 10:e1004652.
80. Smadja DM, Mauge L, Sanchez O, Silvestre JS, Guerin C, Godier A, *et al*. Distinct patterns of circulating endothelial cells in pulmonary hypertension. *Eur Respir J* 2010;36:1284–1293.
81. Vitali SH, Hansmann G, Rose C, Fernandez-Gonzalez A, Scheid A, Mitsialis SA, *et al*. The Sugen 5416/hypoxia mouse model of pulmonary hypertension revisited: long-term follow-up. *Pulm Circ* 2014;4:619–629.
82. Gomez-Arroyo JG, Farkas L, Alhussaini AA, Farkas D, Kraskauskas D, Voelkel NF, *et al*. The monocrotaline model of pulmonary hypertension in perspective. *Am J Physiol Lung Cell Mol Physiol* 2012;302: L363–L369.
83. Dean A, Nilsen M, Loughlin L, Salt IP, MacLean MR. Metformin reverses development of pulmonary hypertension via aromatase inhibition. *Hypertension* 2016;68:446–454.
84. Savai R, Al-Tamari HM, Sedding D, Kojonazarov B, Muecke C, Teske R, *et al*. Pro-proliferative and inflammatory signaling converge on FoxO1 transcription factor in pulmonary hypertension. *Nat Med* 2014;20: 1289–1300.
85. Nwankwo N, Zhang Z, Wang T, Collins C, Resta L, Ermisch S, *et al*. Phase I study of enzastaurin and bevacizumab in patients with advanced cancer: safety, efficacy and pharmacokinetics. *Invest New Drugs* 2013;31:653–660.
86. Schmidinger M, Szczylik C, Sternberg CN, Kania M, Kelly CS, Decker R, *et al*. Dose escalation and pharmacokinetics study of enzastaurin and sunitinib versus placebo and sunitinib in patients with metastatic renal cell carcinoma. *Am J Clin Oncol* 2012;35:493–497.
87. Teicher BA, Alvarez E, Menon K, Esterman MA, Considine E, Shih C, *et al*. Antiangiogenic effects of a protein kinase Cβ-selective small molecule. *Cancer Chemother Pharmacol* 2002;49:69–77.
88. Podar K, Raab MS, Zhang J, McMillin D, Breitkreutz I, Tai YT, *et al*. Targeting PKC in multiple myeloma: in vitro and in vivo effects of the novel, orally available small-molecule inhibitor enzastaurin (LY317615. HCl). *Blood* 2007;109:1669–1677.
89. Nair AB, Jacob S. A simple practice guide for dose conversion between animals and human. *J Basic Clin Pharm* 2016;7:27–31.
90. Bianchi F, Magnifico A, Olgiati C, Zanesi N, Pekarsky Y, Tagliabue E, *et al*. FHIT-proteasome degradation caused by mitogenic stimulation of the EGF receptor family in cancer cells. *Proc Natl Acad Sci USA* 2006;103:18981–18986.
91. Pichiorri F, Okumura H, Nakamura T, Garrison PN, Gasparini P, Suh SS, *et al*. Correlation of fragile histidine triad (Fhit) protein structural features with effector interactions and biological functions. *J Biol Chem* 2009;284:1040–1049.